Computer simulation study of the permeability of a porous sediment model

R. B. Pandey[1,2] and Jeffrey L. Becklehimer[1,3]
[1]*The Program in Scientific Computing, University of Southern Mississippi, Hattiesburg, Mississippi 39406-5046*
[2]*Department of Physics and Astronomy, University of Southern Mississippi, Hattiesburg, Mississippi 39406-5046*
[3]*Naval Research Laboratory, Stennis Space Center, Mississippi 39529*
(Received 29 August 1994)

A computer simulation model is used to study the permeability of fluid flow through porous media generated by the random distribution of the sediments in a two-dimensional lattice. Fluid particles are confined to pore space with the sediments forming the rigid barriers at the pore boundaries. An interaction between the fluid particles and the pore substrate is introduced to incorporate the additional drag in the pore space. The pressure gradient causes a bias to drive the fluid and the Metropolis algorithm is used to hop the fluid particles. The permeability of this system is studied as a function of the global pressure, the concentration of the fluid particles, and the porosity. The permeability shows a nonmonotonic dependence on the fluid concentration and on the driving bias. The fluid particles exhibit unusual transport behavior as the ramification of the porous media is enhanced and the bias is increased.

PACS number(s): 47.55.Mh, 64.75.+g, 83.70.Hq, 91.50.Jc

Studying fluid flow through porous media [1–6] has attracted considerable interest in marine geosciences for a long time with varied applications such as oil exploration, sedimentation processes, spreading of hazardous waste on the sea floor, etc. Distribution of the sediments determines the physical and chemical properties such as the viscoelastic nature of the sediment network, physisorption, and deposition of various species on the pore boundaries formed by sediments. A variety of heterogeneous substrates emerge due to various sedimentation processes involving streams, ocean currents, waves, wind, gravity, etc. [7]. The structure of the porous matrix depends not only on the type of sediments (i.e., particles with various shapes and size distributions) and their interactions, but also on these sediment processes. Furthermore, many of the parameters of these sediment processes (i.e., pressure gradient, flow velocity field, etc.) vary with time. Thus, the structural analysis of pores [8,9] itself constitutes a large area of investigation. Taking into account the ramification of the pores, however, poses one of the major difficulties in understanding the fluid flow through the heterogeneous sediments [9]. Analytical methods are severely limited due to their intractability in handling the nature of nonlinearities in inhomogeneities in such systems. Computer simulations [2,6] on the other hand may be useful in taking into account some of the nonlinearities, although they are limited to idealized model systems. We present here a computer simulation model to study fluid flow through a porous system.

We consider a two-dimensional discrete lattice. Monodisperse sediments (i.e., the sediment particles of uniform shape and size comparable to lattice constant) are then distributed randomly in the lattice with no more than one particle per lattice site. Furthermore, the sediments remain immobile throughout the simulation. The empty sites constitute the pores, which are defied as the clusters of nearest neighbor empty sites. Thus, the random distribution of sediments generates a rigid porous media in which the size of the pores depends on the concentration (i.e., the volume fraction) of the sediments [9]. The volume fraction of the pore space p_s (i.e., the porosity) is defined as the ratio of the number of pore sites to the total number of lattice sites; the volume fraction of the sediments is $1-p_s$. The larger the p_s, the larger the probability of forming large pores. At smaller p_s, not only do we obtain smaller pores but the pores become isolated if we reduce p_s below a certain value—the percolation threshold p_{sc} of the pores [8]. The size and shape of the pores and related geometrical quantities depends on the percolation mechanism [9]. We will restrict ourselves here to the rigid pores formed by random distribution of the monodisperse sediments.

Fluid particles are the placed in pore space of the host matrix; a pore site cannot be occupied by more than one fluid particle. Avoiding the multiple occupancy of a pore site by the fluid particles takes into account the hard-core interactions among the particles. In fact, we consider a short range (nearest neighbor) repulsive interaction among the particles as described below. The amount of fluid in the pores is governed by the concentration p of the fluid particles, which is the fraction of the pore sites occupied by fluid particles. Unlike sediment particles, fluid particles are mobile. A fluid particle may hop to a neighboring pore site; however, it cannot cross the sediment sites. In other words, the sediment sites act as an infinite barrier for the transport of fluid particles. Since we are interested in a global fluid flow, we will restrict ourselves to a high pore volume fraction (i.e., p_s above p_{sc}) in order to obtain infinite connected channels of pores (i.e., the channels across the sample).

In addition to stochastic diffusion of fluid particles (see below), we also implement a global bias produced by the pressure gradient as follows. We set up a bias probability B with $0.25 < B < 0.5$, such that each fluid particle attempts to choose a neighboring hopping site along the

 ©1995 The American Physical Society

$+x$ direction with the probability B, and a neighboring site along the $-x$ direction with probability $0.5-B$. There is no bias along the y direction in which each fluid particle attempts to choose a hopping site in the $+y$ and the $-y$ directions with equal probability (0.25). The bias drives the particles pushing along the x direction, but the hopping is eventually governed by the energetics of the system as we will soon see.

The sediment barriers and the driving bias compete with each other in the transport of the fluid particles. Apart from the geometrical barriers of the sediments causing retardation of the fluid flow, the presence of other elements such as air, waste, or foreign species other than the fluid particles may also add to drag. The effect of viscosity due to the latter is effectively considered via incorporating an attractive interaction between the particles and the empty pore sites. We assign a unit positive charge density ($\rho_p=1$) to each fluid particle and a negative charge density (ρ_s) to each substrate (i.e., empty) pore site, with zero density to sediment sites. The interaction energy is described by

$$E=\sum_{ij}\rho_i\rho_j\ , \tag{1}$$

where ρ_i is the charge density at site i and ρ_j is that at site j; the summation is restricted to nearest neighbor sites. Note that $\rho_i=1$ for the fluid particles and $\rho_i=\rho_s$ for the substrate density. The effect of viscosity within the pores can be varied by varying the interaction energy by varying ρ_s: We consider here two values $\rho_s=-1$ and -2.

We use a combination of direct and importance sampling techniques [10]: the direct sampling to select the direction of the move with the biased probability B and the Metropolis algorithm of the Monte Carlo method to move the fluid particles as follows. We select a particle say at site i and one at its neighboring site j according to the bias probability B. If site j is an empty pore site, then we evaluate the energy E_1 of the particle at site i and energy E_2 of the particle in a configuration in which the particle (i) and the pore site (j) have exchanged their positions. The change in energy $\Delta E=E_2-E_1$ is then evaluated. If ΔE is less than or equal to zero, then we move the particle finally from site i to site j. However, if ΔE is greater than zero, then we move the particle with a Boltzmann distribution $\exp(-\Delta E/k_BT)$, where k_B is the Boltzmann constant and T is the temperature. T is regarded as an effective temperature due to agitation of the system: We keep T constant with $k_BT=1$ throughout the simulation. An attempt to move each fluid particle once is defined as one Monte Carlo Step time. We perform the simulation for a sufficiently large number of time steps to achieve a steady state. Periodic boundary conditions are imposed to move the particles across the edges. During the simulation, we keep track of various physical quantities such as rms displacement of each fluid particle and that of their center of mass, flux of the particles, energy, etc. These simulations are repeated, starting from new initial configurations, for a number of independent runs to gain a reliable estimate of the various physical quantities for different values of biased fields, pore volume fraction p_s, and the concentration of fluid particles.

Most of the simulations were performed on a 100×100 lattice, although we have used different size lattices to check for severe finite size effects. As many as 100 independent samples were used for a fixed bias, pore volume fraction, and the concentration of the fluid particles. The pressure gradient is applied along the x direction; therefore, a net flux of fluid particles along the direction of pressure ($+x$) is expected. The flux entering the sample at the first column must be equal to the flux exiting at the opposite end in order to satisfy the conservation of mass (continuity equation for the fluid flow). Figure 1 shows a typical variation of the mass transfer versus time (along the $+x$ direction) for various concentration of fluid at the bias $B=0.30$. A linear increase of the flux with time is reached in a rather short time particularly at small fluid concentrations, which shows that our system is in the steady sate. From the rate of mass flow (i.e., the mass current) along the pressure gradient, one can estimate the permeability

$$j=\sigma\times\nabla P\ , \tag{2}$$

where j is the current density and ∇P is the pressure gradient, which is proportional to B here; σ is defined as an effective permeability. In our study, we use the last ten data points (in Fig. 1) to evaluate σ in the steady state. We have studied in detail the variation of the permeability, power-law dependence of the rms displacement of each fluid particle, and that of their center of mass with time, and energy with the pore volume fraction (p_s), concentration of the fluid particles, and the strength of the pressure bias. In order to show our worst finite size effects, we present a fluid flux versus time plot in Fig. 2 for various porosities in the regime where the pores are highly ramified (with the fraction of the pore sites close to percolation threshold) for 100×100 and 200×200 samples. The system has reached the steady state for all the data sets. Apart from a larger flux with the larger lattice, the qualitative features remain unchanged by in-

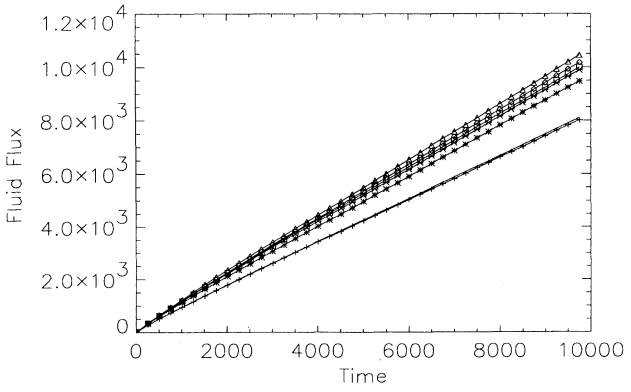

FIG. 1. Flow (mass) flux vs time with the porosity $p_s=0.70$, bias $B=0.3$, $p=0.2$ (+), 0.3 (asterisk), 0.4 (×), 0.5 (square), 0.6 (triangle), 0.7 (diamond),and 0.8 (solid line) with $\rho_s=-1$. 100×100 lattice was used with ten independent samples.

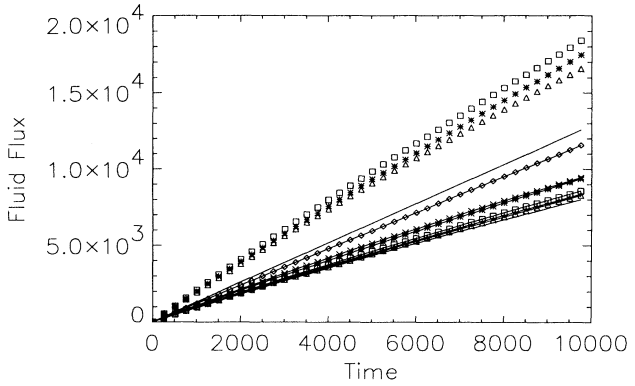

FIG. 2. Fluid flux vs time at the bias $B=0.3$ and fluid concentration $p=0.5$ for various porosity $p_s=0.591$ (+), 0.593 (lower most solid line), 0.595 (triangle), 0.597 (square), 0.599 (×), 0.600 (asterisk), 0.700 (diamond), and 0.800 (the upper most solid line) for 100×100 sample. The upper most disconnected data sets were generated with the sample size 200×200 with the porosity $p_s=0.592$ (asterisk), 0.595 (triangle), and 0.598 (square). Ten independent samples were used with both samples.

creasing the lattice size. Since the current density $j=(\text{slope})/L$ in Fig. 2, a large slope with a larger lattice is not unexpected.

The charge density of the empty sites is fixed for all concentrations of fluid particles. The variation of permeability with the concentration at various bias and porosities is shown in Fig. 3 for $\rho_s=-1$. We immediately note that the permeability depends nonmonotonically on the concentration of the fluid at a fixed value of the bias and the porosity (p_s). On increasing the fluid concentration from low to high values (i.e., $p=0.20-0.8$), the rise in permeability in the low concentration regime is followed by a decline in the high concentration regime. Despite the large fluctuations in data points at low porosity ($p_s=0.60$) in Fig. 3(a), the variations in the data points at the higher porosity ($p_s=0.70$) clearly show a nonmonotonic behavior even with ten independent runs. The curves are smoothed out with 100 samples as shown in Fig. 3(b). These curves exhibit a conclusive nonmonotonic dependence at all porosity including $p_s=0.60$. Note that the statistical error in the data points is reduced considerably on increasing the number of samples [compare Fig. 3(a) and 3(b)]; the error bar in the data points is comparable to the size of the symbols in the data with the 100 samples. At a fixed pressure bias, we observe a higher permeability at larger porosity, i.e., at the bias $B=0.3$; the permeability is higher at $p_s=0.70$ than that at $p_s=0.6$, as expected.

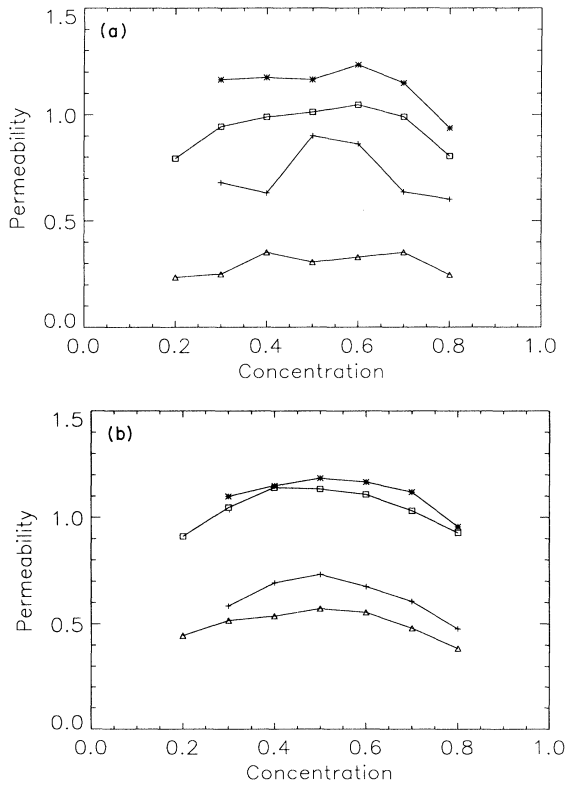

FIG. 3. Permeability vs fluid concentration at bias $B=0.3$ and porosity $p_s=0.6$ (+), 0.7 (asterisk), and $B=0.4$, and $p_s=0.6$ (triangle) and 0.7 (square) with the same statistics as in Fig. 1 with 10 samples (a) and 100 samples (b).

One may ask what is the relevance of the concentration dependence of the permeability? We would like to address this question qualitatively as follows. The hopping of fluid particles depends strongly on their concentration especially in the dense regime. Thus, the variation in concentration may be used to change the quality of the fluid. For example, the mixture of contaminants such as sewer in water may reduce the flow (and the permeability) considerably due to its higher viscosity. The concentration of the fluid particle in conjunction with the fluid substrate interaction can be used to consider the effect of both the quality of the fluid and the viscosity of the medium.

In Table I, we present data for the permeability for various porosities at bias $B=0.3$ and fluid concentration $p=0.5$ for the two sample sizes $L=100$ and 200. We see that the data for the permeability with different size samples were in accordance with no severe finite size effect within the range of fluctuations. The pores are highly ramified around the porosity $p_s=0.592$ (near percolation threshold of the pore sites); therefore, large fluctuations

TABLE I. Variation of permeability with the porosity for sample size $L=100$ and 200 at the bias $B=0.3$ and fluid concentration $p=0.50$.

Porosity	Permeability	Size (L)
0.591	0.7891	100
0.592	0.8455	200
0.593	0.7514	100
0.595	0.7688	200
0.595	0.8013	100
0.597	0.8130	100
0.598	0.8808	200
0.599	0.8710	100
0.600	0.9002	100
0.700	1.1648	100
0.800	1.2890	100

are expected in the evaluation of the permeability in this region, especially with a small number of independent samples (ten). The larger permeability at $p_s=0.591$ rather than that at $p_s=0.593$, as an example, is purely due to statistical fluctuations, which can be reduced by increasing the number of samples as we saw above. At higher porosity, the data becomes less fluctuating as the ramifications in the pore structure are reduced.

The change in permeability, however, seems to depend on the pressure gradient: The higher the gradient, the larger the change in permeability on varying the porosity (Fig. 3). Note a large decrease in permeability at $p_s=0.6$ when we increase the bias from 0.3 to 0.4. (The site percolation threshold [8] for the pore sites is about $p_{sc}=0.592$ and the porosity must be greater than this for the global fluid flow.) The porous media is very ramified at such a low porosity and even a small pressure bias reduces the permeability. The permeability is zero at p_s below p_{sc} when the pores are isolated. At a fixed porosity ($p_s=0.7$) and fluid concentration $p=0.3$, the permeability first increases on increasing the pressure gradient (B above 0.25) but begins to decline on increasing B beyond a certain characteristic value (B_c about 0.275) (see Fig. 4). Above this characteristic value, the bias begins to compete with the sediment barrier. The characteristic value of the bias seems to depend on the fluid concentration as well as on the porosity; the smaller the porosity, the lower the characteristic value of the bias. Although we observe a maxima in permeability at the characteristic value B_c about 0.30 at the fluid concentration $p=0.60$, this trend is not as clear at all concentrations (i.e., $p=0.4$, 0.5, 0.8). Thus, we see that permeability depends strongly on the porosity and pressure gradient. While the permeability decreases continuously on decreasing the porosity, the interplay between the sediment barriers and the bias leads to a nonmonotonic dependence of the permeability on the pressure gradient.

On increasing the drag, i.e., the interaction between the substrate (empty pore sites) and the fluid particles, we find that permeability drops abruptly (see Fig. 5). However, the nature of its dependence on the fluid concentration does not change significantly on increasing the drag.

We know that permeability is a cooperative quantity

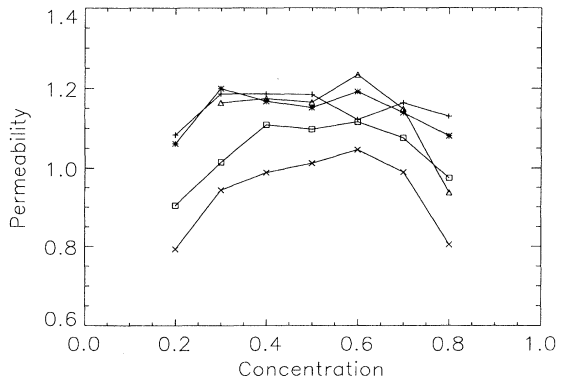

FIG. 4. Permeability vs fluid concentration at porosity $p_s=0.7$ for various bias, $B=0.260$ (+), 0.275, (asterisk), 0.300 (triangle), 0.350 (square), 0.400(×). Same statistics as Fig. 1.

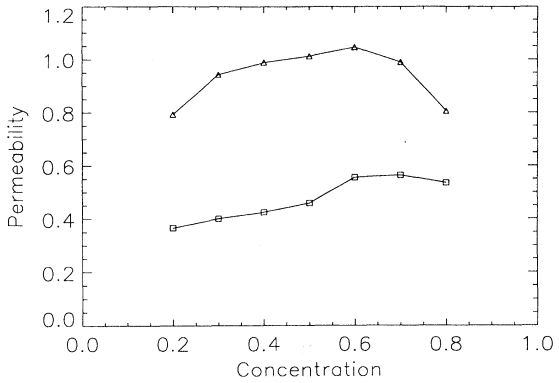

FIG. 5. Permeability vs fluid concentration at porosity $p_s=0.7$ and bias $B=0.4$ with the substrate interaction density $\rho_s=-1$ (triangle) and -2 (square). Same statistics as Fig. 1.

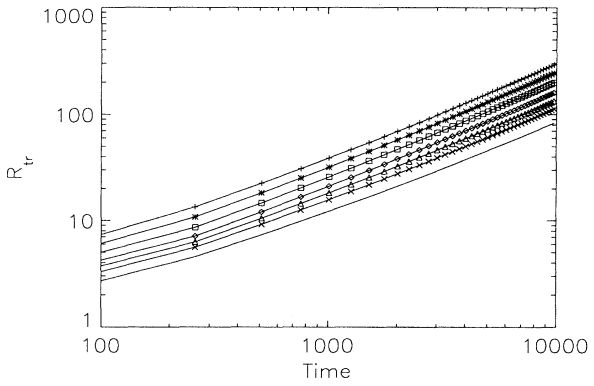

FIG. 6. RMS displacement of each fluid particle (R_{tr}) vs time at porosity $p_s=0.7$ and bias $B=0.4$ for various fluid concentrations $p=0.2$ (+), 0.3 (asterisk), 0.4 (square), 0.5 (diamond), 0.6 (triangle), 0.7 (×), and 0.8 (solid line). Same statistics as Fig. 1.

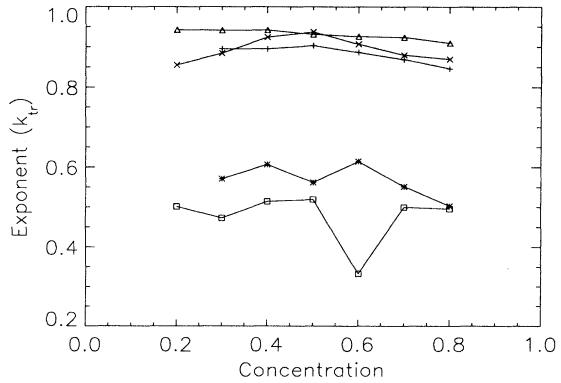

FIG. 7. Power-law exponent k_{tr} for the variation of the rms displacement of fluid particle (R_{tr}) with time at bias $B=0.3$ and porosity $p_s=0.6$ (asterisk), 0.7 (+), and bias $B=0.4$, $p_s=0.6$ (square), and 0.7 (triangle). All of these data sets are taken with the substrate density $\rho_s=-1$ except the one at $p_s=0.7$ and $B=0.4$ shown by crosses, which was taken with $\rho_S=-2$. Same statistics as Fig. 1.

that emerges from the transport properties of the individual fluid particles in the heterogeneous porous media. It may, therefore, be useful to see how the individual particles (i.e., the tracers) behave by analyzing their rms displacements R_{tr}, which is the average rms displacement traversed by each particle. Figure 6 shows a typical plot of R_{tr} versus time (t) for various p and p_s on a log-log scale. Such a good linear dependence of R_{tr} on t, particularly in the long time (asymptotic) regime suggests a power-law behavior, i.e., $R_{tr} \sim t^{k_{tr}}$ where k_{tr} is an exponent. We have studied such power laws in detail; the variation of the power-law exponent k_{tr} with the fluid concentration is presented in Fig. 7 for various values of the pressure gradient and porosity.

We know that a diffusing particle shows a driftlike motion (i.e., $k_{tr}=1$) in the presence of a global bias in a homogeneous space. Even in a highly porous media with $p_s=0.70$, here the value of k_{tr} never approached 1. In fact, it lies between 0.80 and 0.95 for the bias $B=0.30$ and 0.40 with the substrate intensity $\rho_s=-1$ and -2. At low porosity (and high ramification), $p_s=0.60$, on the other hand, the value of the exponent k_{tr} drops down significantly; some data points are even below 0.5. A lower value of k_{tr} implies slower motion of the individual particles. Note further, that k_{tr} has lower values at the higher bias at $p_s=0.60$. Increasing the bias reduces the mobility at such a high ramified porous media due to competition between the bias and the barriers. This results in a decline of the permeability on increasing the bias as we have seen above. We should point out that the power-law exponent k_{tr} is nonuniversal as it depends on the porosity and the bias.

In summary, we have presented a computer simulation model to study the fluid flow through a porous media. The porous media is created by the random distribution of sediments as in site percolation, and the fluid is modeled by discrete particles, which are restricted to pores. The effective viscosity within the pore is considered via an interaction between the fluid particles and the pore substrate. An external pressure gradient is applied to drive the fluid across this porous media and the permeability is evaluated. The effect of porosity, concentration of fluid, driving bias, and viscosity is studied. We find that permeability depends nonmonotonically on the concentration of the fluid. For some fluid concentration at a fixed porosity, the permeability increases on increasing the bias until a certain characteristic value (B_c) above which it decreases; the characteristic bias seems to depend strongly on the porosity with higher B_c at the higher porosity. It also depends on the concentration p; however, this dependence is not clear at this stage. Thus, for a model porous media we can predict how the permeability depends on the pressure gradient, porosity, and drag. One may consider a more realistic model for the porous media generated by the network of sediments of certain shape and size distributions with elastic properties, multicomponent fluid, effect of transient bias including shock, and various type of drags in this model. We plan to consider some of these aspects in our continued effort.

We would like to thank Joe Gettrust, Dennis Lindwall, and Dietrich Stauffer for discussions. Major support from the Navy-ASEE summer faculty research program is acknowledged by R.B.P. along with partial support from a NSF-EPSCoR grant. This work was supported in part by a grant from the DOD HPC shared Resource Center, Wright Pattern Air Force Base, for the HPC time on Paragon.

[1] M. Sahimi, Rev. Mod. Phys. **65**, 1393 (1993) and references therein, *Application of Percolation* (Taylor & Francis, London, 1994).
[2] A. Cancelliere, C. Cahng, E. Foti, D. H. Rothman, and S. Succi, Phys. Fluids A **2**, 2085 (1990).
[3] D. H. Rothman, Geophysics **53**, 509 (1988).
[4] D. H. Rothman, J. Geophys. Res. **95**, 8663 (1990).
[5] C. Baudet, J.-P. Hulin, P. Lallemand, and D. d'Humieres, Phys. Fluids A **1**, 507 (1989).
[6] G. A. Kohring, Physica A **186**, 97 (1992).
[7] J. K. Mitchell, *Fundamentals of Soil Behavior* (Wiley, New York, 1976).
[8] D. Stauffer and A. Aharony, *Introduction to Percolation Theory* (Taylor & Francis, London, 1992).
[9] J. L. Becklehimer and R. B. Pandey, J. Stat. Phys. **75**, 765 (1994).
[10] *Application of Monte Carlo Simulation in Statistical Physics,* edited by K. Binder (Springer-Verlag, Berlin, 1986).